Noise-induced Parrondo's paradox in discrete-time quantum walks

Zbigniew Walczak [*] and Jarosław H. Bauer [†]

*Department of Theoretical Physics, Faculty of Physics and Applied Informatics, University of Lodz,
Pomorska 149/153, 90-236 Lodz, Poland*

Parrondo's paradox refers to the apparently paradoxical effect whereby two or more dynamics in which a given quantity decreases are combined in such a way that the same quantity increases in the resulting dynamics. We show that noise can induce Parrondo's paradox in one-dimensional discrete-time quantum walks with deterministic periodic as well as aperiodic sequences of two-state quantum coins where this paradox does not occur in the absence of noise. Moreover, we show how the noise-induced Parrondo's paradox affects the time evolution of quantum entanglement for such quantum walks.

I. INTRODUCTION

In 1996, Parrondo [1] proposed a game-theoretic model of the flashing Brownian ratchet introduced by Ajdari and Prost [2]. The original Parrondo game consists of two games A and B, in which a player's capital increases or decreases by one at each game run. In game A, the capital increases by one with probability $0.5 - \varepsilon$ and decreases by one with probability $0.5 + \varepsilon$, that is, the player wins with probability $0.5 - \varepsilon$ and loses with probability $0.5 + \varepsilon$, where $\varepsilon = 0.005$. In game B, if the capital is a multiple of three, then the player wins with probability $0.1 - \varepsilon$ and loses with probability $0.9 + \varepsilon$, but if the capital is not a multiple of three, then the player wins with probability $0.75 - \varepsilon$ and loses with probability $0.25 + \varepsilon$. If each of these games is played individually (i.e., $AAAA\ldots$ or $BBBB\ldots$), then the Parrondo game results in losing, that is, the average capital is a decreasing function of the number of runs. However, if they are played randomly or in a certain deterministic sequence (e.g., $ABBABB\ldots$, $ABBAABBA\ldots$, etc.), then the Parrondo game results in winning, that is, the average capital is an increasing function of the number of runs. A detailed explanation of the original Parrondo game, in terms of Markov chains, can be found in Refs. [3–5]. This counterintuitive phenomenon was called Parrondo's paradox [6,7]. In general, the term Parrondo's paradox refers to the situation where two or more dynamics in which a given quantity decreases are combined in such a way that the same quantity increases in the resulting dynamics [3]. In the past two decades, Parrondo's paradox, called also the Parrondo's effect, has received attention not only in game theory where different variants of Parrondo's games were studied [3–5,8–19] but also in various areas of research, ranging from chaos and nonlinear dynamics [20–28], ecology and evolutionary biology [29–41], economics and social dynamics [42–47], to quantum

information [48–68]. Comprehensive reviews on Parrondo's paradox can be found in Refs. [69–73].

In the field of quantum information, Parrondo's paradox has been studied mainly within the framework of discrete-time quantum walks [51,53,54,56–58,60–68]. A discrete-time coined quantum walk on an infinite one-dimensional lattice (DTQW) is a bipartite quantum system consisting of a coin and a walker moving along the lattice [74–76]. The walker-coin system dynamics is driven by an operator which, at each time step, first performs a transformation of the coin state and then, depending on the resulting state, shifts the walker from one position on the lattice to another.

The DTQWs with deterministic periodic sequence of two two-state quantum coins (representing games A and B) that exhibit Parrondo's effect have been presented in Refs. [56,57]. However, in both cases this effect disappears after a certain relatively small number of time steps. Interestingly, the long-lasting Parrondo's effect, called also the genuine Parrondo's effect, can occur in DTQWs with deterministic periodic sequence of two three- and four-state quantum coins [61,62] as well as in DTQWs with deterministic periodic sequence of two entangled two-state quantum coins [60]. Until recently, it was believed that DTQWs with deterministic periodic sequence of two two-state quantum coins exhibiting the genuine Parrondo's effect do not exist. However, it has been shown both theoretically and experimentally that this is not the case [63–65,68]. Moreover, it has been shown that the genuine Parrondo's effect can occur also in DTQWs with deterministic aperiodic sequence of two two-state quantum coins [66] and in DTQWs with deterministic aperiodic as well as periodic sequence of three two-state quantum coins [67].

Although it is well known that noise can induce counterintuitive phenomena in nonlinear dynamical systems, until now the occurrence of the genuine Parrondo's effect in DTQWs has been studied only in the noiseless regime. In this work, we demonstrate, by providing explicit examples, that noise can induce the genuine Parrondo's effect in DTQWs with deterministic periodic as well as aperiodic sequences of two-state quantum coins where this effect does not occur in the

----

*zbigniew.walczak@uni.lodz.pl
†jaroslaw.bauer@uni.lodz.pl

absence of noise. Moreover, we show how, in these cases, the noise-induced genuine Parrondo's effect affects the time evolution of the walker-coin quantum entanglement.

II. DTQWs

A DTQW is defined on the Hilbert space $\mathcal{H} = \mathcal{H}_w \otimes \mathcal{H}_c$, where $\mathcal{H}_w$ is the walker Hilbert space spanned by the orthonormal states $\{|x\rangle : x \in \mathbb{Z}\}$ representing the walker's position on the lattice while $\mathcal{H}_c$ is the coin Hilbert space spanned by the orthonormal states $\{|0\rangle, |1\rangle\}$. At time step t, the walker-coin system is in the following state [76]

$$|\psi(t)\rangle = \sum_x |x\rangle (a_x(t)|0\rangle + b_x(t)|1\rangle), \qquad (1)$$

where the probability amplitudes $a_x(t)$ and $b_x(t)$ satisfy the normalization condition $\sum_x (|a_x(t)|^2 + |b_x(t)|^2) = 1$. The one-step time evolution of the walker-coin system

$$|\psi(t+1)\rangle = U|\psi(t)\rangle \qquad (2)$$

is governed by the unitary operator

$$U = S(I \otimes C(q, \theta, \phi)), \qquad (3)$$

where

$$S = \sum_x |x-1\rangle\langle x| \otimes |0\rangle\langle 0| + \sum_x |x+1\rangle\langle x| \otimes |1\rangle\langle 1| \qquad (4)$$

is the conditional shift operator acting on $\mathcal{H}$, I is the identity operator acting on $\mathcal{H}_w$, and

$$C(q, \theta, \phi) = \begin{pmatrix} \sqrt{q} & \sqrt{1-q}e^{i\theta} \\ \sqrt{1-q}e^{i\phi} & -\sqrt{q}e^{i(\theta+\phi)} \end{pmatrix}, \qquad (5)$$

with $0 \leqslant q \leqslant 1$, $\theta \geqslant 0$ and $\phi \leqslant \pi$ is the coin operator acting on $\mathcal{H}_c$ [76].

At time step t, the walker position probability distribution has the form

$$p(x, t) = |a_x(t)|^2 + |b_x(t)|^2, \qquad (6)$$

while the walker average position and the walker position variance are given by

$$\langle x \rangle(t) = \sum_x x p(x, t), \qquad (7)$$

$$\sigma^2(t) = \sum_x x^2 p(x, t) - \left(\sum_x x p(x, t) \right)^2, \qquad (8)$$

respectively. Interestingly, if the walker-coin initial state has the form $|\psi(0)\rangle = |0\rangle(a_0(0)|0\rangle + b_0(0)|1\rangle)$, then the walker position probability distribution $p(x, t)$, the walker average position $\langle x \rangle(t)$ and the walker position variance $\sigma^2(t)$ do not depend on ϕ but only on q, θ, $a_0(0)$ and $b_0(0)$ [77,78]. However, if $a_0(0) = 1$ and $b_0(0) = 0$, then they depend only on q [77,78]. Moreover, if $a_0(0) = 1$ and $b_0(0) = 0$ and $1/2 \leqslant q \leqslant 1$, then the average position of the walker at time step t is nonpositive and reads [77,78]

$$\langle x \rangle(t) = -q^{t-1} \left[(2q-1)t + \sum_{k=1}^{\left[\frac{t-1}{2}\right]} \sum_{\gamma=1}^{k} \sum_{\delta=1}^{k} \left(\frac{q-1}{q} \right)^{\gamma+\delta} \frac{(t-2k)^2 \kappa_{\gamma,\delta,t,k}}{\gamma\delta} ((2q-1)t + \gamma + \delta) \right], \qquad (9)$$

where $\kappa_{\gamma,\delta,t,k} = \binom{k-1}{\gamma-1}\binom{k-1}{\delta-1}\binom{t-k-1}{\gamma-1}\binom{t-k-1}{\delta-1}$ while $[\frac{t-1}{2}]$ denotes the maximal integer smaller than or equal to $\frac{t-1}{2}$.

At time step t, the walker-coin quantum entanglement can be quantified by entanglement negativity [79,80]

$$\mathcal{N}(t) = \frac{\left\| \rho(t)^{T_w} \right\|_1 - 1}{2}, \qquad (10)$$

where the superscript T_w denotes the partial transpose of the walker-coin state $\rho(t)$ with respect to the first subsystem, and $||\mathcal{O}||_1 = \text{Tr}(\sqrt{\mathcal{O}^\dagger \mathcal{O}})$ is the trace norm of an operator $\mathcal{O}$. The entanglement negativity $\mathcal{N}(t)$, being the absolute value of the sum of all negative eigenvalues of $\rho(t)^{T_w}$, ranges from 0 to 1/2 for the walker-coin system. For the walker-coin separable states it takes the value 0, while for the walker-coin maximally entangled states it takes the value 1/2. Unlike entanglement entropy $\mathcal{S}_E(t)$, being the von Neumann entropy of the coin state at time step t [81], the entanglement negativity quantifies quantum entanglement present not only in pure but also in mixed states of the walker-coin system. The entanglement entropy ranges from 0 for the walker-coin separable states to 1 for the walker-coin maximally entangled states [81]. Although

both measures of quantum entanglement take their minimum and maximum values for the same type of states, the entanglement negativity differs from the entanglement entropy for all other pure entangled states [82], as the entanglement entropy and the entanglement negativity are connected in the following way:

$$2\mathcal{S}_E(t) = (1 + d(t))(1 - \log_2[1 + d(t)])$$
$$+ (1 - d(t))(1 - \log_2[1 - d(t)]), \qquad (11)$$

where $d(t) = \sqrt{1 - 4\mathcal{N}^2(t)}$ and the convention that $0\log_2 0 = 0$ is adopted. Interestingly, if the walker-coin initial state has the form $|\psi(0)\rangle = |0\rangle(a_0(0)|0\rangle + b_0(0)|1\rangle)$, then the entanglement negativity $\mathcal{N}(t)$ does not depend on ϕ but only on q, θ, $a_0(0)$ and $b_0(0)$ [see Fig. 9(a)]. Moreover, if $a_0(0) = 1$ and $b_0(0) = 0$, then it depends only on q [see Fig. 9(b)].

To show that noise can induce the genuine Parrondo's effect in DTQWs with deterministic periodic as well as aperiodic sequences of two-state quantum coins where this effect does not occur in the absence of noise, let us consider two
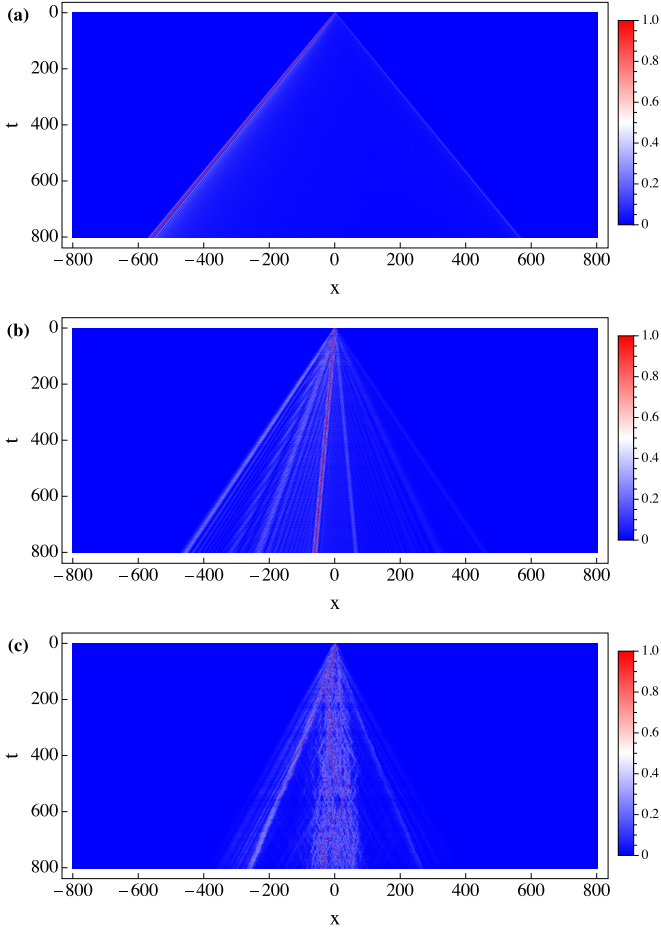
FIG. 1. The space-time evolution of $p(x, t) / \max_x p(x, t)$. The plot (a) is for noiseless DTQWs with the coin operator C_A and C_B, respectively, understood as DTQWs with the period-one sequence of the coin operators C_A and C_B, respectively. The plots (b) and (c) are for noiseless DTQWs with deterministic periodic and aperiodic sequences of the coin operators C_A and C_B given by Eqs. (15) and (16), respectively.

DTQWs with the coin operators respectively given by

$$C_A \equiv C(1/2, 0, 0), \tag{12}$$

$$C_B \equiv C(1/2, 3\pi/4, \pi/2), \tag{13}$$

where in each of the above DTQWs a separable state of the form

$$|\psi(0)\rangle = |0\rangle|0\rangle \tag{14}$$

is the walker-coin initial state. Since q has the same form for each of the above DTQWs, understood respectively as DTQWs with the period-one sequence of the coin operators C_A and C_B, therefore at a given time step t the walker position probability distribution $p(x, t)$, the walker average position $\langle x \rangle(t)$, the walker-coin quantum entanglement $\mathcal{N}(t)$ and the walker position variance $\sigma^2(t)$ are exactly the same for each of the above DTQWs [see Figs. 1(a), 2(a), 3(a), and 4(a)]. The walker position probability distribution for each of the above DTQWs has a bias toward negative values of x [see Fig. 1(a)] such that the walker average position is
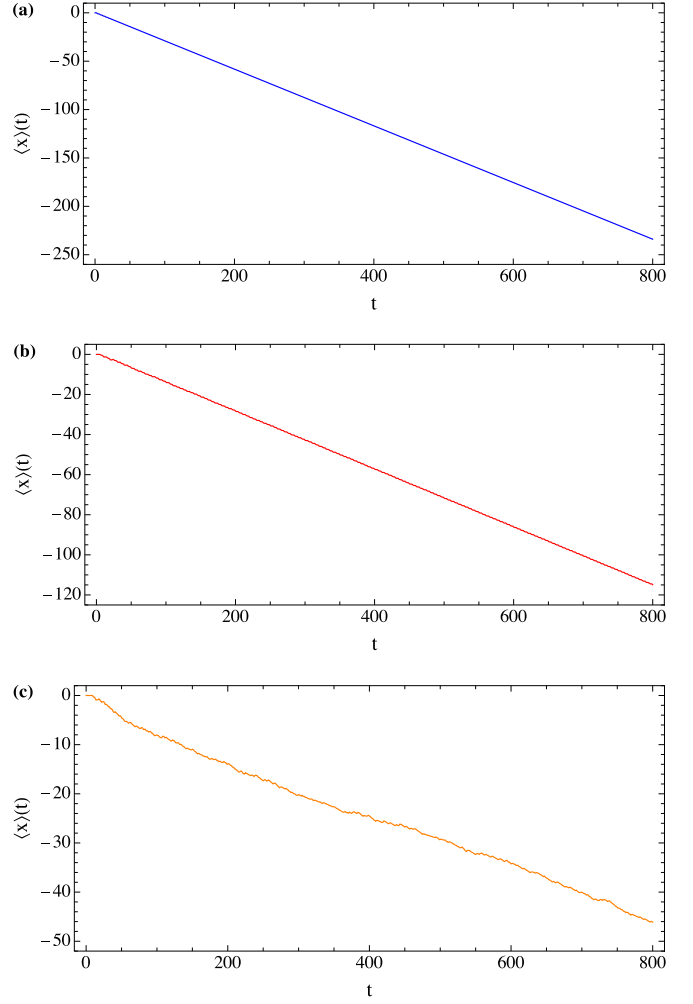

FIG. 2. The time evolution of the walker average position. The plot (a) is for noiseless DTQWs with the coin operator C_A and C_B, respectively, understood as DTQWs with the period-one sequence of the coin operators C_A and C_B, respectively. The plots (b) and (c) are for noiseless DTQWs with deterministic periodic and aperiodic sequences of the coin operators C_A and C_B given by Eqs. (15) and (16), respectively.

nonpositive [see Fig. 2(a)]. For each of the above DTQWs, the time evolution of the walker-coin quantum entanglement quantified by the entanglement negativity is in agreement with the result showing that, in the case of such DTQWs, $\lim_{t \to \infty} \mathcal{N}(t) \approx 0.455089$ [see Fig. 3(a)], since $\lim_{t \to \infty} \mathcal{S}_E(t) \approx 0.872429$ [81] and the connection (11) between $\mathcal{S}_E(t)$ and $\mathcal{N}(t)$ holds. Moreover, the walker position variance for each of the above DTQWs is ballistic, that is, it grows quadratically with time, $\sigma^2(t) \propto t^2$ [see Fig. 4(a)].

Let us introduce now two DTQWs with the following sequences of the coin operators C_A and C_B:

$$C_A C_B C_B C_B C_B C_A C_B C_B C_B C_B C_A C_B C_B C_B C_B \ldots, \tag{15}$$

$$C_A C_B C_B C_B C_B C_B C_B C_B C_B C_B C_A C_B C_B C_B C_B C_A \ldots, \tag{16}$$

where C_A and C_B are defined by Eqs. (12) and (13), and in each of the above DTQWs the walker-coin initial state has the form defined by Eq. (14). Let us note that the first sequence is
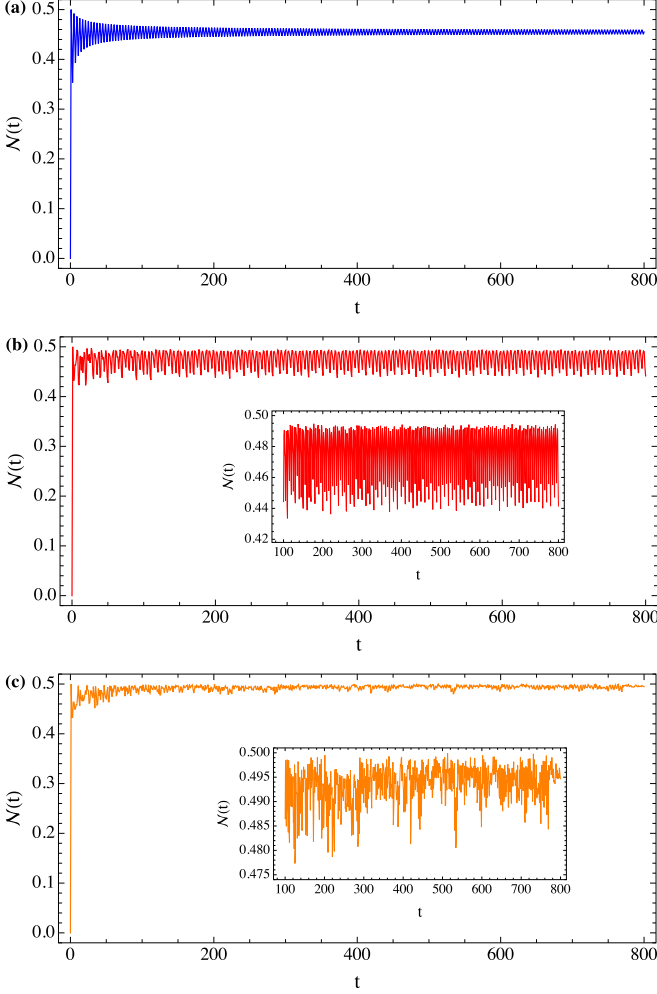
FIG. 3. The time evolution of the walker-coin quantum entanglement. The plot (a) is for noiseless DTQWs with the coin operator C_A and C_B, respectively, understood as DTQWs with the period-one sequence of the coin operators C_A and C_B, respectively. The plots (b) and (c) are for noiseless DTQWs with deterministic periodic and aperiodic sequences of the coin operators C_A and C_B given by Eqs. (15) and (16), respectively.

periodic with period 5 while the second sequence is aperiodic, and moreover each of the above sequences is deterministic. The second sequence is deterministic because the coin operators $C_B C_B C_B C_B$ and C_A are at positions of prime and nonprime numbers, respectively. The walker position probability distribution $p(x, t)$ for each of the above DTQWs has a bias toward negative values of x [see Figs. 1(b) and 1(c)] such that the average position of the walker $\langle x \rangle(t)$ is nonpositive [see Figs. 2(b) and 2(c)]. Thus, none of the above DTQWs exhibits the genuine Parrondo's effect. The time evolution of the walker-coin quantum entanglement $\mathcal{N}(t)$ for these DTQWs [see Figs. 3(b) and 3(c)] shows that, in these cases, the walker-coin quantum entanglement is greater, on average, than in the cases of DTQWs with the period-one sequence of the coin operators C_A and C_B, respectively [see Fig. 3(a)]. Moreover, the walker position variance $\sigma^2(t)$ for each of the above DTQWs is ballistic [see Figs. 4(b) and 4(c)]. In the next section, we show that the genuine Parrondo's effect can be induced by adding noise into the walker-coin system.
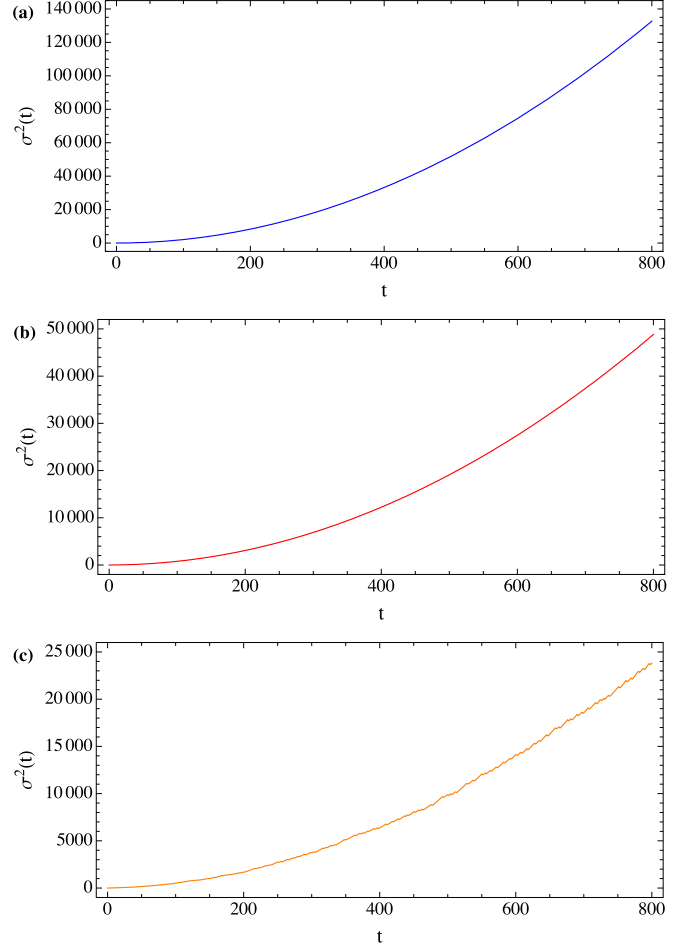

FIG. 4. The time evolution of the walker position variance. The plot (a) is for noiseless DTQWs with the coin operator C_A and C_B, respectively, understood as DTQWs with the period-one sequence of the coin operators C_A and C_B, respectively. The plots (b) and (c) are for noiseless DTQWs with deterministic periodic and aperiodic sequences of the coin operators C_A and C_B given by Eqs. (15) and (16), respectively.

III. PARRONDO'S PARADOX INDUCED BY NOISE

To demonstrate that the genuine Parrondo's effect can be induced by noise, let us consider now DTQWs in which the coin subsystem is subject to the noise that has no direct effect on the walker subsystem [83] (a comprehensive review of noisy DTQWs can be found in Ref. [84]). For such DTQWs, each evolution step starts with a quantum channel acting on the coin subsystem, and then the unitary operator U, defined by Eq. (3), is applied to the walker-coin system [83]. At time step t, the action of a given quantum channel $\mathcal{E}$ on the walker-coin state $\rho(t)$ can be expressed as a trace-preserving quantum operation $(I \otimes \mathcal{E})\rho(t)$ written in the operator-sum representation [85]

$$(I \otimes \mathcal{E})\rho(t) = \sum_k (I \otimes E_k)\rho(t)(I \otimes E_k)^\dagger, \qquad (17)$$

where Kraus operators E_k acting on $\mathcal{H}_c$ satisfy the following condition $\sum_k E_k^\dagger E_k = I$. Therefore, in the case of such noisy DTQWs, the one-step time evolution of the walker-coin
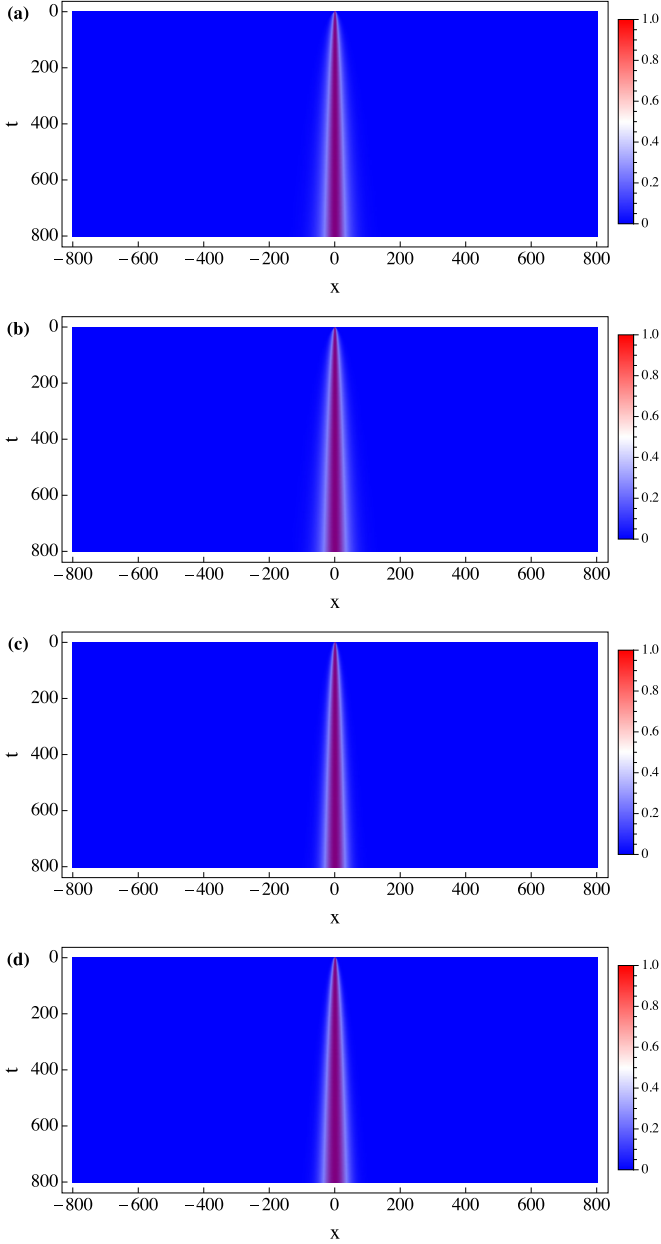
FIG. 5. The space-time evolution of $p(x,t)/\max_x p(x,t)$. The plots (a) and (b) are for noisy DTQWs with the coin operator C_A and C_B, respectively, understood as DTQWs with the period-one sequence of the coin operators C_A and C_B, respectively. The plots (c) and (d) are for noisy DTQWs with deterministic periodic and aperiodic sequences of the coin operators C_A and C_B given by Eqs. (15) and (16), respectively.

FIG. 6. The time evolution of the walker average position. The plots (a) and (b) are for noisy DTQWs with the coin operator C_A and C_B, respectively, understood as DTQWs with the period-one sequence of the coin operators C_A and C_B, respectively. The plots (c) and (d) are for noisy DTQWs with deterministic periodic and aperiodic sequences of the coin operators C_A and C_B given by Eqs. (15) and (16), respectively.

system is given by

$$\rho(t+1) = U[(I \otimes \mathcal{E})\rho(t)]U^\dagger. \qquad (18)$$

At time step t, the walker position probability distribution has the form

$$p(x,t) = \mathrm{Tr}[(|x\rangle\langle x| \otimes I)\rho(t)], \qquad (19)$$

where I is the identity operator acting on $\mathcal{H}_c$, and the walker average position and the walker position variance are given by Eqs. (7) and (8), respectively.
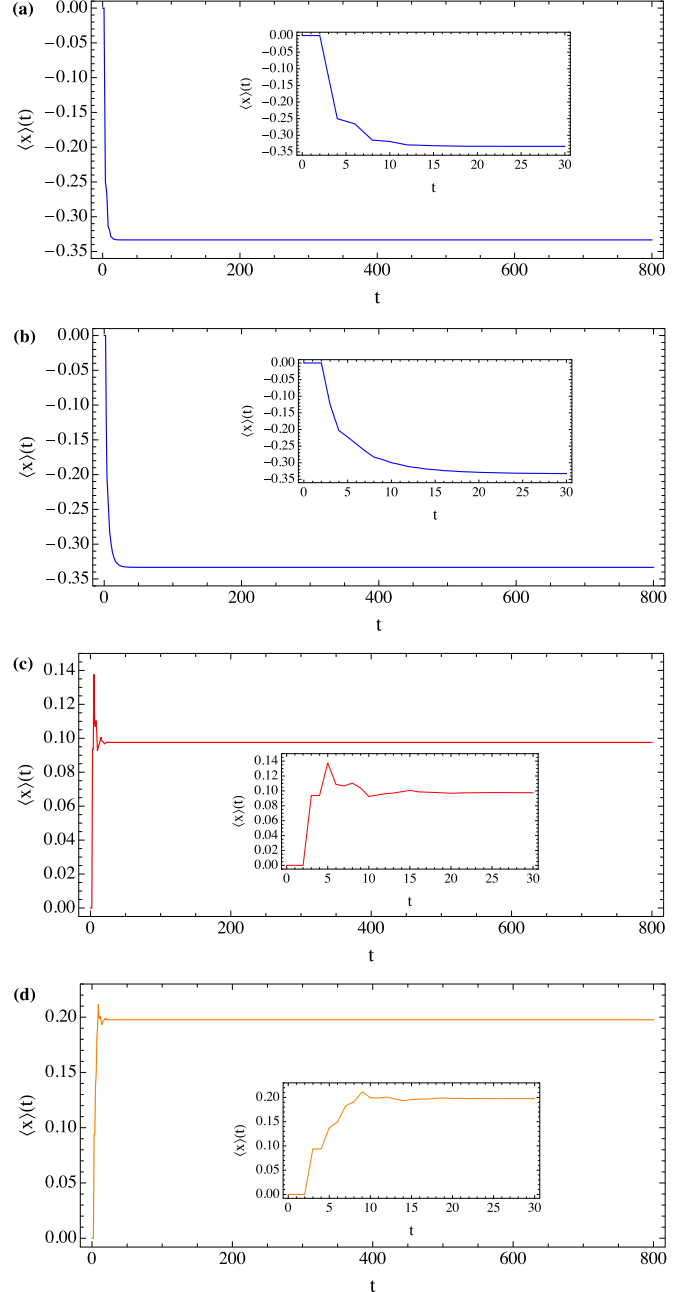
Let us assume that $\mathcal{E}$ is bit-flip quantum channel represented by the Kraus operators $E_1 = \sqrt{1-p}\,I$ and $E_2 = \sqrt{p}\,\sigma_1$, where p is the flipping probability and σ_1 is the first Pauli matrix [85]. This means that now each evolution step starts with flipping the coin basis states from $|0\rangle$ to $|1\rangle$, and vice versa, with probability p or the coin basis states are left untouched with probability $1-p$, and then the unitary operator U, defined by Eq. (3), is applied to the walker-coin
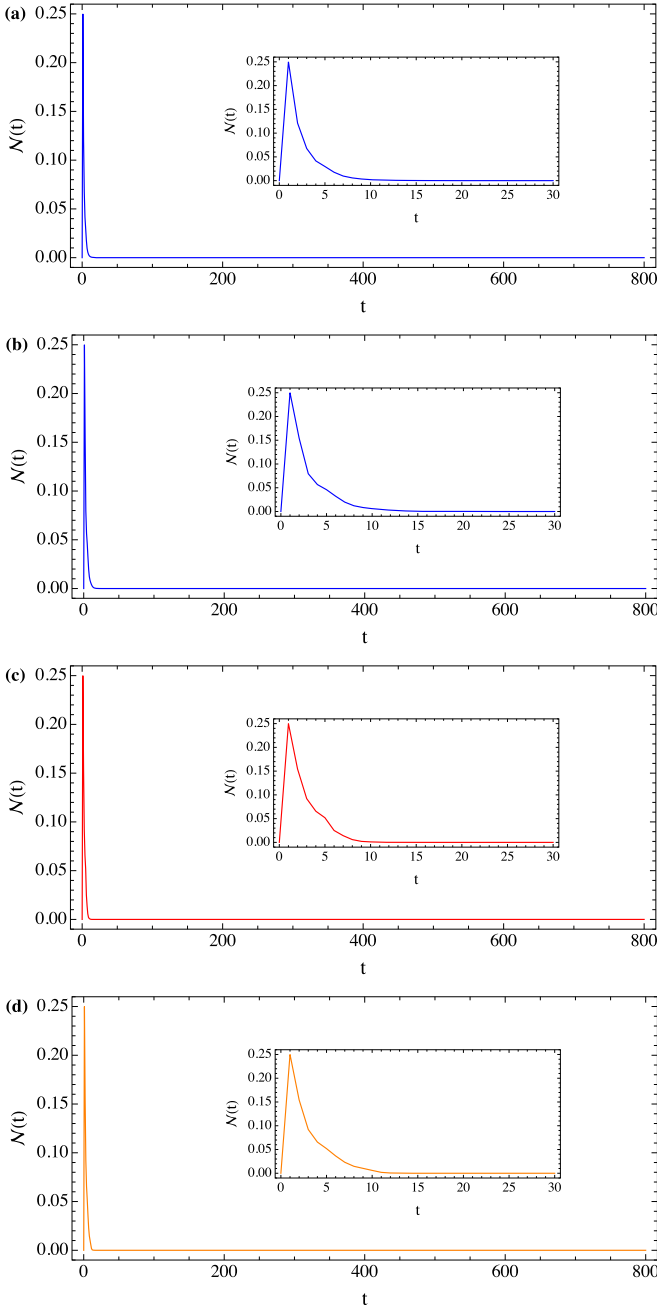
FIG. 7. The time evolution of the walker-coin quantum entanglement. The plots (a) and (b) are for noisy DTQWs with the coin operator C_A and C_B, respectively, understood as DTQWs with the period-one sequence of the coin operators C_A and C_B, respectively. The plots (c) and (d) are for noisy DTQWs with deterministic periodic and aperiodic sequences of the coin operators C_A and C_B given by Eqs. (15) and (16), respectively.
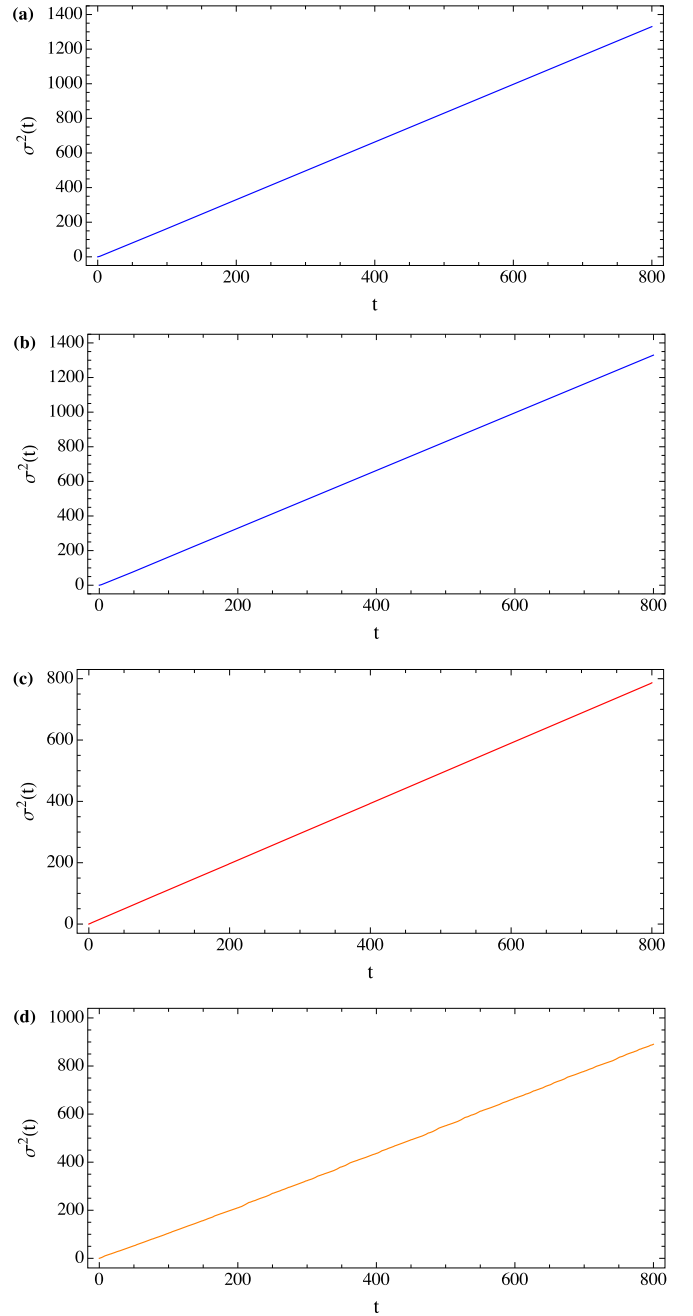

FIG. 8. The time evolution of the walker position variance. The plots (a) and (b) are for noisy DTQWs with the coin operator C_A and C_B, respectively, understood as DTQWs with the period-one sequence of the coin operators C_A and C_B, respectively. The plots (c) and (d) are for noisy DTQWs with deterministic periodic and aperiodic sequences of the coin operators C_A and C_B given by Eqs. (15) and (16), respectively.

system. In the case of such noisy DTQWs, the one-step time evolution of the walker-coin system takes the following form

$$\rho(t+1) = U[(I \otimes \mathcal{E})\rho(t)]U^{\dagger}$$

$$= \sum_k U[(I \otimes E_k)\rho(t)(I \otimes E_k)^{\dagger}]U^{\dagger}$$

$$= U[(I \otimes \sqrt{1-p}\,I)\rho(t)(I \otimes \sqrt{1-p}\,I)^{\dagger}]U^{\dagger}$$

$$+ U[(I \otimes \sqrt{p}\,\sigma_1)\rho(t)(I \otimes \sqrt{p}\,\sigma_1)^{\dagger}]U^{\dagger}$$

$$= (1-p)\,U\rho(t)U^{\dagger} + p\,U(I \otimes \sigma_1)\rho(t)(I \otimes \sigma_1)U^{\dagger},$$
(20)

due to Eqs. (18) and (17). Moreover, in the case of such noisy DTQWs, if the walker-coin initial state has the form defined by Eq. (14), then the walker position probability distribution
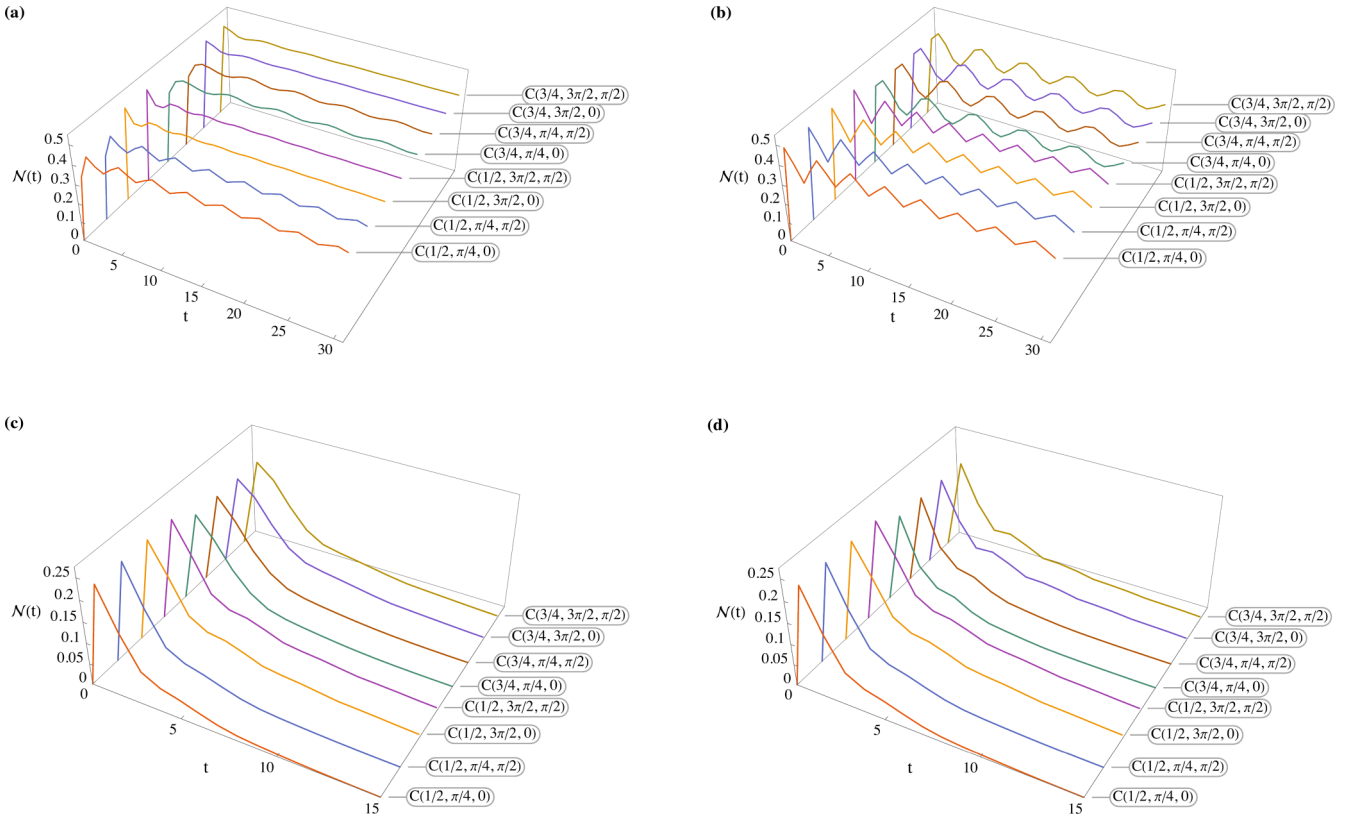
FIG. 9. The time evolution of the walker-coin quantum entanglement. The plot (a) is for noiseless DTQWs with the coin operator $C(q, \theta, \phi)$, understood as DTQWs with the period-one sequence of the coin operator $C(q, \theta, \phi)$, where the walker-coin initial state has the form $|\psi(0)\rangle = |0\rangle(\frac{1}{\sqrt{2}}|0\rangle + \frac{1}{\sqrt{2}}|1\rangle)$. The plot (b) is for noiseless DTQWs with the coin operator $C(q, \theta, \phi)$, where the walker-coin initial state has the form defined by Eq. (14). The plot (c) is for noisy DTQWs with the coin operator $C(q, \theta, \phi)$, where $p = 0.25$ and the walker-coin initial state has the form defined by Eq. (14). The plot (d) is for noisy DTQWs with the coin operator $C(q, \theta, \phi)$, where $p = 0.75$ and the walker-coin initial state has the form defined by Eq. (14).

$p(x, t)$, the walker average position $\langle x \rangle(t)$, the walker position variance $\sigma^2(t)$ and the walker-coin quantum entanglement $\mathcal{N}(t)$ do not depend on ϕ but only on q, θ and p [see Figs. 11, 12, and 9(c)–9(d)]. Furthermore, in the case of noiseless DTQWs, they depend only on q [see Figs. 10 and 9(b)].

Let us assume further that each of the four DTQWs considered in the previous section is subject to the bit-flip noise with $p = 0.25$. Since only θ has a different form for each of the first two noisy DTQWs, therefore at a given time step t, the walker position probability distribution $p(x, t)$, the walker average position $\langle x \rangle(t)$, the walker-coin quantum entanglement $\mathcal{N}(t)$ and the walker position variance $\sigma^2(t)$ cannot be the same for these noisy DTQWs, although the difference may be very small [see Figs. 5(a), 5(b), 6(a), 6(b), 7(a), 7(b), and 8(a), 8(b)]. This difference can increase if not only θ has a different form for each of these DTQWs, but also q. Applying the framework of Ref. [83], it can be shown that for the first two noisy DTQWs $\lim_{t\to\infty} \langle x \rangle(t) = -1/3$ [see Figs. 6(a) and 6(b)]. Moreover, within this framework, it can be demonstrated that for noisy DTQWs with the period-one sequence of the coin operator $C(q, \theta, \phi)$ and the walker-coin initial state defined by Eq. (14) the walker position variance is diffusive for all $p > 0$, that is, it grows linearly with time, $\sigma^2(t) \propto t$,

like in the case of classical random walks [see Figs. 8(a) and 8(b)].

Let us note now that for noisy DTQWs with deterministic periodic and aperiodic sequences of the coin operators C_A and C_B defined by Eqs. (15) and (16), respectively, the walker position probability distribution $p(x, t)$ has a bias toward positive values of x [see Figs. 5(c) and 5(d)] such that the average position of the walker $\langle x \rangle(t)$ is nonnegative and tends to a constant value asymptotically [see Figs. 6(c) and 6(d)]. Therefore, each of these noisy DTQWs exhibits the genuine Parrondo's effect, although their noiseless counterparts do not exhibit such effect, which demonstrates that the genuine Parrondo's effect can be induced by noise. It is important to emphasize that all results regarding the genuine Parrondo's effects, whether noiseless or noise-induced, have been found only by performing numerical simulations because a theory predicting when and why these effects may occur in the DTQWs scenario has not yet been developed [56,57,60–64,66–68]. Interestingly, the walker-coin quantum entanglement $\mathcal{N}(t)$ decays asymptotically which shows that the genuine Parrondo's effect need not be accompanied by the walker-coin quantum entanglement enhancement [see Figs. 7(c) and 7(d)], as it is the case in the noiseless regime [64,66,67]. Moreover, the
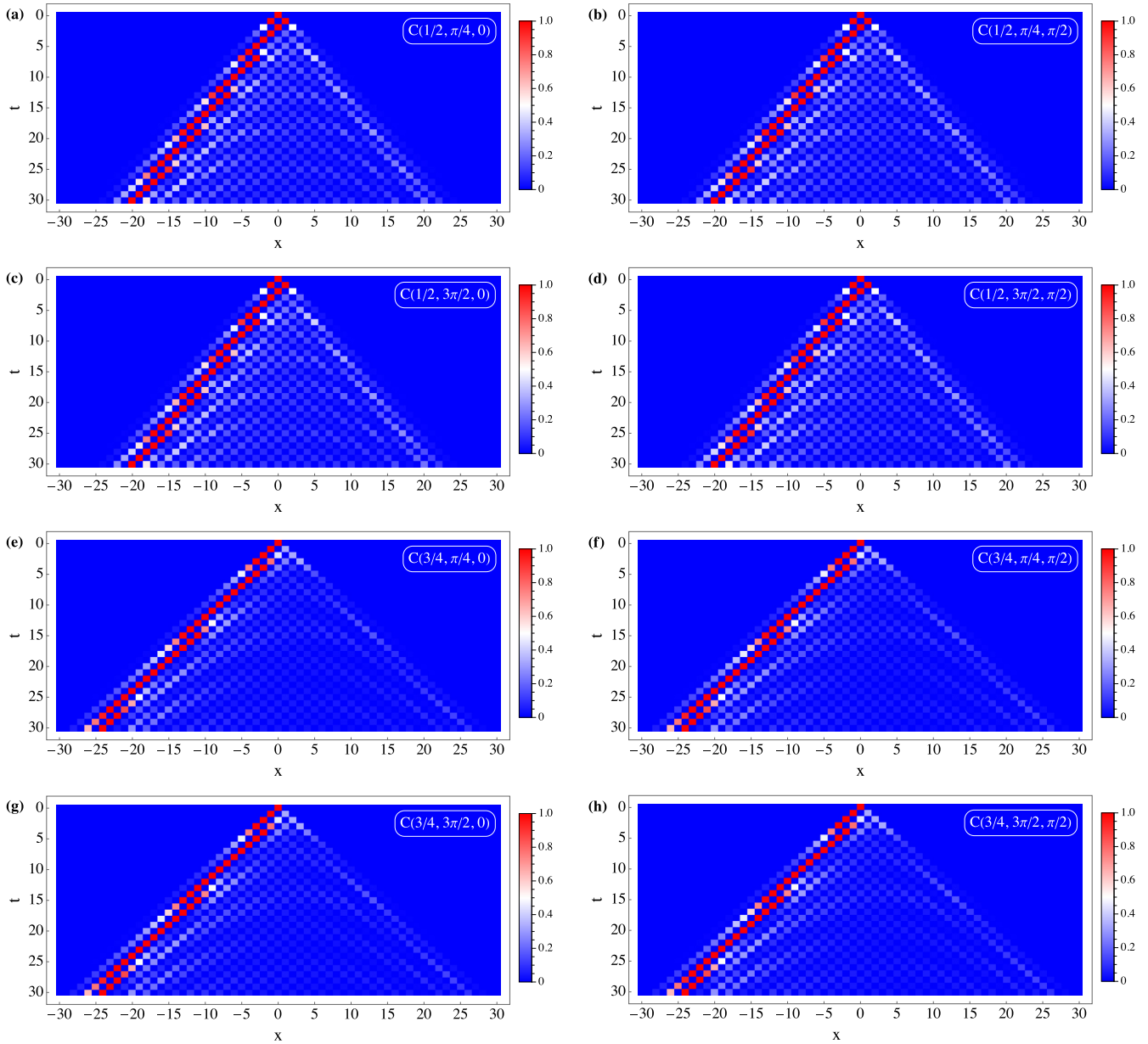
FIG. 10. The space-time evolution of $p(x, t)/ \max_x p(x, t)$. The plots [(a)–(h)] are for noiseless DTQWs with the coin operator $C(q, \theta, \phi)$, understood as DTQWs with the period-one sequence of the coin operator $C(q, \theta, \phi)$, where the walker-coin initial state has the form defined by Eq. (14).

TABLE I. Ratio between the number of the DTQWs exhibiting the noise-induced genuine Parrondo's effect to the number of the all DTQWs for noisy DTQWs with the deterministic periodic sequences of the coin operators C_A and C_B defined by Eqs. (12) and (13), respectively, with a period of length L.

| L	$p = 0.1$	$p = 0.2$	$p = 0.3$	$p = 0.4$	$p = 0.5$	$p = 0.6$	$p = 0.7$	$p = 0.8$	$p = 0.9$
2	0/2	0/2	0/2	0/2	0/2	1/2	1/2	1/2	0/2
3	0/6	0/6	0/6	0/6	0/6	2/6	2/6	2/6	2/6
4	0/14	0/14	1/14	1/14	0/14	1/14	1/14	1/14	0/14
5	0/30	1/30	3/30	3/30	0/30	2/30	2/30	2/30	0/30
6	0/62	1/62	4/62	4/62	0/62	6/62	6/62	6/62	2/62
7	0/126	5/126	12/126	12/126	0/126	14/126	14/126	12/126	6/126
8	1/254	9/254	22/254	22/254	0/254	22/254	22/254	19/254	5/254
9	0/510	15/510	40/510	40/510	0/510	46/510	46/510	39/510	12/510
10	1/1022	30/1022	78/1022	78/1022	0/1022	82/1022	82/1022	68/1022	20/1022
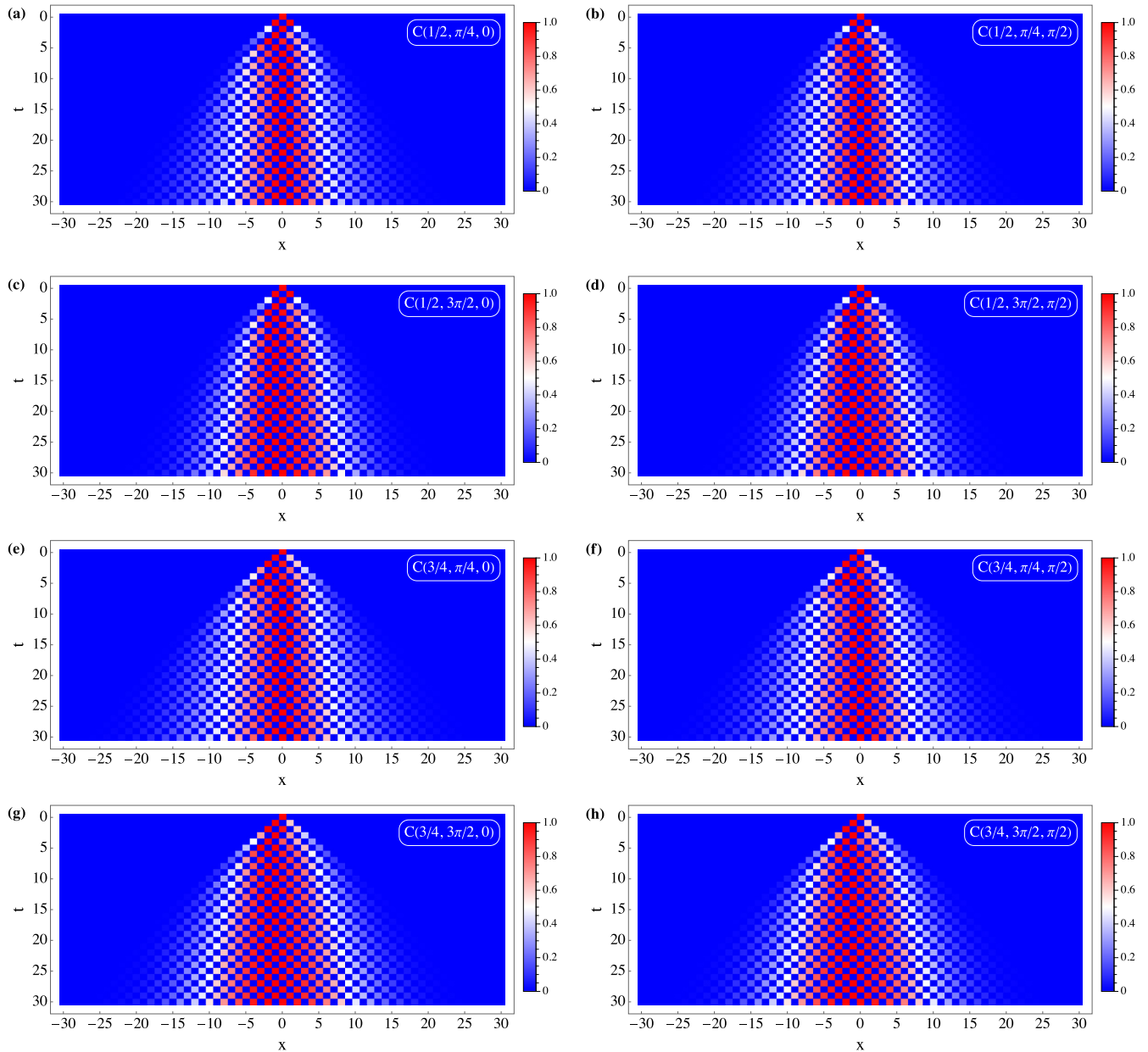
FIG. 11. The space-time evolution of $p(x, t)/\max_x p(x, t)$. The plots [(a)–(h)] are for noisy DTQWs with the coin operator $C(q, \theta, \phi)$, understood as DTQWs with the period-one sequence of the coin operator $C(q, \theta, \phi)$, where $p = 0.25$ and the walker-coin initial state has the form defined by Eq. (14).

walker position variance $\sigma^2(t)$ for each of these noisy DTQWs is diffusive [see Figs. 8(c) and 8(d)]. Furthermore, for these noisy DTQWs, the time evolution of quantum entanglement is very similar, with very small differences within the first fifteen time steps [see Figs. 7(c) and 7(d)]. These differences are so minimal because only θ has a different form for each of the coin operators C_A and C_B [see Eqs. (12) and (13)], and the first fifteen terms of the deterministic periodic and aperiodic sequences of the coin operators C_A and C_B are almost identical [see Eqs. (15) and (16)].

Interestingly, the occurrence of the noise-induced genuine Parrondo's effect is not limited to the case when each of the

four DTQWs considered in the previous section is subject to the bit-flip noise with $p = 0.25$. This effect also occurs when the parameter p is varied in increments of 0.1 from 0.1 to 0.9, specifically for values $p = 0.2, 0.3, 0.4$, with all conclusions regarding the case $p = 0.25$ remaining valid.

In general, the occurrence of the noise-induced genuine Parrondo's effect depends not only on the bit-flip noise strength but also on the forms of the walker-coin initial state, the coin operators and the sequence of the coin operators. Interestingly, for the walker-coin initial state, the sequences of the coin operators and the bit-flip noise considered above, the noise-induced genuine Parrondo's effect occurs not only
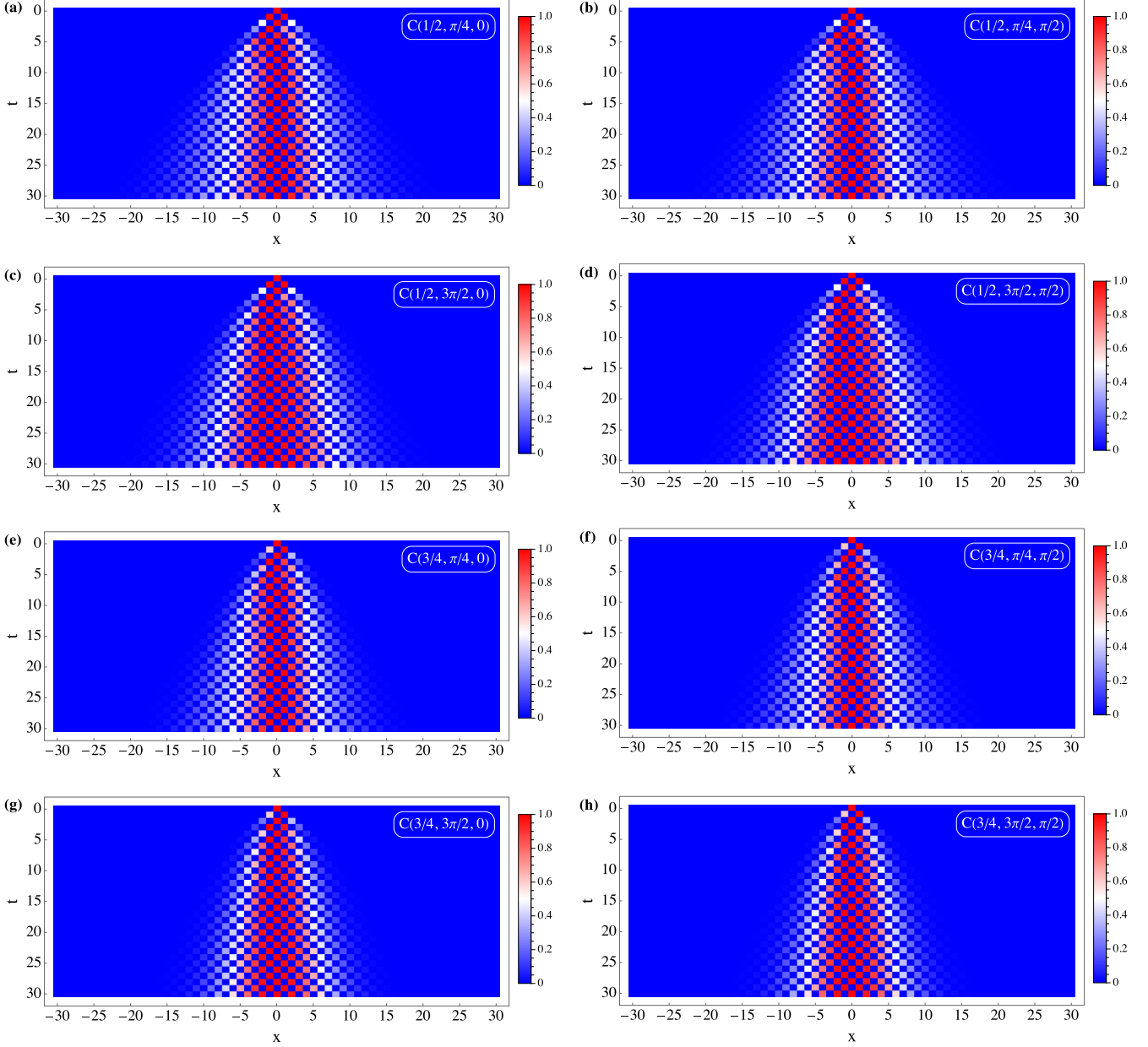
FIG. 12. The space-time evolution of $p(x,t)/\max_x p(x,t)$. The plots [(a)–(h)] are for noisy DTQWs with the coin operator $C(q,\theta,\phi)$, understood as DTQWs with the period-one sequence of the coin operator $C(q,\theta,\phi)$, where $p = 0.75$ and the walker-coin initial state has the form defined by Eq. (14).

for the coin operators C_A and C_B defined by Eqs. (12) and (13) but also for the following ones:

$$C_A \equiv C(1/2, \pi/4, \pi/4), \tag{21}$$

$$C_B \equiv C(1/2, 3\pi/4, 3\pi/4), \tag{22}$$

with all conclusions regarding the case with the coin operators C_A and C_B defined by Eqs. (12) and (13) remaining valid. Therefore, the noise-induced genuine Parrondo's effect can occur for coin operators beyond just those defined by Eqs. (12) and (13). Moreover, for the walker-coin initial state defined by Eq. (14) and both pairs of the coin operators considered above, it can be determined how many DTQWs with the deterministic periodic sequences of the coin operators exhibit

the noise-induced genuine Parrondo's effect, for the selected bit-flip noise strengths (see Tables I and II).

IV. CONCLUSION

We have shown that the genuine Parrondo's effect can occur in the case of DTQWs with deterministic periodic as well as aperiodic sequences of two-state quantum coins subject to noise by providing the first examples of such quantum walks. Moreover, we have shown how the noise-induced genuine Parrondo's effect affects the time evolution of the walker-coin quantum entanglement. More precisely, the noise-induced genuine Parrondo's effect leads to the walker-coin quantum entanglement asymptotic decay which shows that the genuine

TABLE II. Ratio between the number of the DTQWs exhibiting the noise-induced genuine Parrondo's effect to the number of the all DTQWs for noisy DTQWs with the deterministic periodic sequences of the coin operators C_A and C_B defined by Eqs. (21) and (22), respectively, with a period of length L.

L	$p = 0.1$	$p = 0.2$	$p = 0.3$	$p = 0.4$	$p = 0.5$	$p = 0.6$	$p = 0.7$	$p = 0.8$	$p = 0.9$
2	0/2	0/2	0/2	0/2	0/2	2/2	2/2	0/2	0/2
3	0/6	0/6	2/6	2/6	0/6	2/6	2/6	2/6	2/6
4	0/14	0/14	4/14	4/14	0/14	4/14	4/14	2/14	2/14
5	0/30	2/30	8/30	8/30	0/30	8/30	8/30	8/30	0/30
6	0/62	4/62	16/62	16/62	0/62	16/62	16/62	12/62	12/62
7	0/126	8/126	32/126	32/126	0/126	32/126	32/126	26/126	22/126
8	0/254	16/254	62/254	62/254	0/254	64/254	64/254	52/254	40/254
9	6/510	32/510	120/510	120/510	0/510	128/510	128/510	104/510	84/510
10	8/1022	64/1022	246/1022	246/1022	0/1022	254/1022	254/1022	206/1022	162/1022

Parrondo's effect need not be accompanied by the walker-coin quantum entanglement enhancement, as it has been the case in the noiseless regime. Moreover, the occurrence of this effect is connected with the walker dynamics change from ballistic to diffusive. We hope that our results might be experimentally verified in the quantum optics framework and potentially could be helpful in designing new quantum algorithms.

APPENDIX

The problem of how the walker-coin quantum entanglement $\mathcal{N}(t)$ and the walker position probability distribution $p(x, t)$ depend on the walker-coin initial state $|\psi(0)\rangle$ and the parameters q, θ, ϕ and p can be investigated by performing numerical simulations because, in general, this problem is analytically intractable. Our numerical simulations indicate that, in the case of noiseless DTQWs, if the walker-coin initial state has the form $|\psi(0)\rangle = |0\rangle(a_0(0)|0\rangle + b_0(0)|1\rangle)$, then the walker-coin quantum entanglement $\mathcal{N}(t)$ does not depend on ϕ but only on q, θ, $a_0(0)$ and $b_0(0)$. Moreover, if $a_0(0) = 1$ and $b_0(0) = 0$, then the walker-coin quantum entanglement $\mathcal{N}(t)$ and the walker position probability distribution $p(x, t)$ depend only on q. Furthermore, in the case of noisy DTQWs, if $a_0(0) = 1$ and $b_0(0) = 0$, then the walker-coin quantum entanglement $\mathcal{N}(t)$ and the walker position probability distribution $p(x, t)$, and consequently the walker average position $\langle x \rangle(t)$ and the walker position variance $\sigma^2(t)$, do not depend on ϕ but only on q, θ and p. A few of the numerical simulations illustrating these assertions are presented in Figs. 9–12.

[1] J. M. R. Parrondo, Efficiency of Brownian motors, in *Workshop of the EEC HC&M Network on Complexity and Chaos* (ISI Foundation, Torino, Italy, 1996) (unpublished).

[2] A. Ajdari and J. Prost, Drift induced by a spatially periodic potential of low symmetry: Pulsed dielectrophoresis, C. R. Acad. Sci. Paris Série 2 **315**, 1635 (1992).

[3] J. M. R. Parrondo, G. P. Harmer, and D. Abbott, New paradoxical games based on Brownian ratchets, Phys. Rev. Lett. **85**, 5226 (2000).

[4] J. M. R. Parrondo and L. Dinis, Brownian motion and gambling: From ratchets to paradoxical games, Contemp. Phys. **45**, 147 (2004).

[5] L. Dinis, Optimal sequence for Parrondo games, Phys. Rev. E **77**, 021124 (2008).

[6] G. P. Harmer and D. Abbott, Parrondo's paradox, Statist. Sci. **14**, 206 (1999).

[7] G. P. Harmer and D. Abbott, Losing strategies can win by Parrondo's paradox, Nature (London) **402**, 864 (1999).

[8] R. Toral, Cooperative Parrondo's games, Fluct. Noise Lett. **01**, L7 (2001).

[9] L. Dinis and J. M. R. Parrondo, Optimal strategies in collective Parrondo games, Europhys. Lett. **63**, 319 (2003).

[10] R. J. Kay and N. F. Johnson, Winning combinations of history-dependent games, Phys. Rev. E **67**, 056128 (2003).

[11] N.-G. Xie, Y. Chen, Y. Ye, G. Xu, L.-G. Wang, and C. Wang, Theoretical analysis and numerical simulation of Parrondo's paradox game in space, Chaos Solitons Fractals **44**, 401 (2011).

[12] Y. Ye, N.-G. Xie, L. Wang, and Y.-W. Cen, The multi-agent Parrondo's model based on the network evolution, Physica A **392**, 5414 (2013).

[13] K. W. Cheung, H. F. Ma, D. Wu, G. C. Lui, and K. Y. Szeto, Winning in sequential Parrondo games by players with short-term memory, J. Stat. Mech. (2016) 054042.

[14] K. H. Cheong, D. B. Saakian, and R. Zadourian, Allison mixture and the two-envelope problem, Phys. Rev. E **96**, 062303 (2017).

[15] J. M. Koh and K. H. Cheong, New doubly-anomalous Parrondo's games suggest emergent sustainability and inequality, Nonlinear Dyn. **96**, 257 (2019).

[16] J. M. Koh and K. H. Cheong, Generalized solutions of Parrondo's games, Adv. Sci. **7**, 2001126 (2020).

[17] Y. Ye, X.-S. Zhang, L. Liu, and N.-G. Xie, Effects of group interactions on the network Parrondo's games, Physica A **583**, 126271 (2021).

[18] J. W. Lai and K. H. Cheong, Boosting Brownian-inspired games with network synchronization, Chaos Solitons Fractals **168**, 113136 (2023).

[19] J. A. Miszczak, Constructing games on networks for controlling the inequalities in the capital distribution, Physica A **594**, 126997 (2022).

[20] L. Kocarev and Z. Tasev, Lyapunov exponents, noise-induced synchronization, and Parrondo's paradox, Phys. Rev. E **65**, 046215 (2002).

[21] P. Arena, S. Fazzino, L. Fortuna, and P. Maniscalco, Game theory and non-linear dynamics: The Parrondo paradox case study, Chaos Solitons Fractals **17**, 545 (2003).

[22] J. Almeida, D. Peralta-Salas, and M. Romera, Can two chaotic systems give rise to order? Physica D **200**, 124 (2005).

[23] A. Boyarsky, P. Góra, and M. S. Islam, Randomly chosen chaotic maps can give rise to nearly ordered behavior, Physica D **210**, 284 (2005).

[24] J. S. Cánovas, A. Linero, and D. Peralta-Salas, Dynamic Parrondo's paradox, Physica D **218**, 177 (2006).

[25] M.-F. Danca, M. Fečkan, and M. Romera, Generalized form of Parrondo's paradoxical game with applications to chaos control, Int. J. Bifurcation Chaos **24**, 1450008 (2014).

[26] S. A. Mendoza, E. W. Matt, D. R. Guimarães-Blandón, and E. Peacock-López, Parrondo's paradox or chaos control in discrete two-dimensional dynamic systems, Chaos Solitons Fractals **106**, 86 (2018).

[27] J. Cánovas and M. Muñoz-Guillermo, On the dynamics of the *q*-deformed logistic map, Phys. Lett. A **383**, 1742 (2019).

[28] J. Cánovas and M. Muñoz-Guillermo, On the dynamics of a hyperbolic–exponential model of growth with density dependence, Commun. Nonlinear Sci. Numer. Simul. **104**, 106050 (2022).

[29] D. M. Wolf, V. V. Vazirani, and A. P. Arkin, Diversity in times of adversity: Probabilistic strategies in microbial survival games, J. Theor. Biol. **234**, 227 (2005).

[30] F. A. Reed, Two-locus epistasis with sexually antagonistic selection: A genetic Parrondo's paradox, Genetics **176**, 1923 (2007).

[31] K. H. Cheong, Z. X. Tan, N.-G. Xie, and M. C. Jones, A paradoxical evolutionary mechanism in stochastically switching environments, Sci. Rep. **6**, 34889 (2016).

[32] Z. X. Tan and K. H. Cheong, Nomadic-colonial life strategies enable paradoxical survival and growth despite habitat destruction, eLife **6**, e21673 (2017).

[33] A. Fotoohinasab, E. Fatemizadeh, and H. Pezeshk, Denoising of genetic switches based on Parrondo's paradox, Physica A **493**, 410 (2018).

[34] J. M. Koh, N.-G. Xie, and K. H. Cheong, Nomadic-colonial switching with stochastic noise: Subsidence-recovery cycles and long-term growth, Nonlinear Dyn. **94**, 1467 (2018).

[35] Z.-X. Tan and K. H. Cheong, Periodic habitat destruction and migration can paradoxically enable sustainable territorial expansion, Nonlinear Dyn. **98**, 1 (2019).

[36] K. H. Cheong, T. Wen, and J. W. Lai, Relieving cost of epidemic by Parrondo's paradox: A COVID-19 case study, Adv. Sci. **7**, 2002324 (2020).

[37] N. Ejlali, H. Pezeshk, Y. P. Chaubey, M. Sadeghi, A. Ebrahimi, and A. Nowzari-Dalini, Parrondo's paradox for games with three players and its potential application in combination therapy for type II diabetes, Physica A **556**, 124707 (2020).

[38] S. Jia, J. W. Lai, J. M. Koh, N. G. Xie, and K. H. Cheong, Parrondo effect: Exploring the nature-inspired framework on periodic functions, Physica A **556**, 124714 (2020).

[39] Z.-X. Tan, J. M. Koh, E. V. Koonin, and K. H. Cheong, Predator dormancy is a stable adaptive strategy due to Parrondo's paradox, Adv. Sci. **7**, 1901559 (2020).

[40] T. Wen, E. V. Koonin, and K. H. Cheong, An alternating active-dormitive strategy enables disadvantaged prey to outcompete the perennially active prey through Parrondo's paradox, BMC Biology **19**, 168 (2021).

[41] T. Wen, K. H. Cheong, J. W. Lai, J. M. Koh, and E. V. Koonin, Extending the lifespan of multicellular organisms via periodic and stochastic intercellular competition, Phys. Rev. Lett. **128**, 218101 (2022).

[42] R. Spurgin and M. Tamarkin, Switching investments can be a bad idea when Parrondo's paradox applies, J. Behav. Finance **6**, 15 (2005).

[43] H. F. Ma, K. W. Cheung, G. C. Lui, D. Wu, and K. Y. Szeto, Effect of information exchange in a social network on investment, Comput. Econ. **54**, 1491 (2019).

[44] Y. Ye, X. R. Hang, J. M. Koh, J. A. Miszczak, K. H. Cheong, and N. G. Xie, Ratcheting based on neighboring niches determines lifestyle, Nonlinear Dyn. **98**, 1821 (2019).

[45] Y. Ye, X. R. Hang, J. M. Koh, J. A. Miszczak, K. H. Cheong, and N.-G. Xie, Passive network evolution promotes group welfare in complex networks, Chaos Solitons Fractals **130**, 109464 (2020).

[46] J. W. Lai and K. H. Cheong, Evaluation of single-prioritization voting systems in controlled collective Parrondo's games, Nonlinear Dyn. **107**, 2965 (2022).

[47] J. W. Lai and K. H. Cheong, Risk-taking in social Parrondo's games can lead to Simpson's paradox, Chaos Solitons Fractals **158**, 111911 (2022).

[48] D. A. Meyer and H. Blumer, Parrondo games as lattice gas automata, J. Stat. Phys. **107**, 225 (2002).

[49] A. P. Flitney, J. Ng, and D. Abbott, Quantum Parrondo's games, Physica A **314**, 35 (2002).

[50] A. P. Flitney and D. Abbott, Quantum models of Parrondo's games, Physica A **324**, 152 (2003).

[51] A. P. Flitney, D. Abbott, and N. F. Johnson, Quantum walks with history dependence, J. Phys. A **37**, 7581 (2004).

[52] P. Gawron and J. A. Miszczak, Quantum implementation of Parrondo's paradox, Fluct. Noise Lett. **05**, L471 (2005).

[53] J. Košik, J. A. Miszczak, and V. Bužek, Quantum Parrondo's game with random strategies, J. Mod. Opt. **54**, 2275 (2007).

[54] D. Bulger, J. Freckleton, and J. Twamley, Position-dependent and cooperative quantum Parrondo walks, New J. Phys. **10**, 093014 (2008).

[55] L. Chen, C.-F. Li, M. Gong, and G.-C. Guo, Quantum Parrondo game based on a quantum ratchet effect, Physica A **389**, 4071 (2010).

[56] A. P. Flitney, Quantum Parrondo's games using quantum walks, arXiv:1209.2252.

[57] M. Li, Y.-S. Zhang, and G.-C. Guo, Quantum Parrondo's games constructed by quantum random walks, Fluct. Noise Lett. **12**, 1350024 (2013).

[58] Ł. Pawela and J. Sładkowski, Cooperative quantum Parrondo's games, Physica D **256-257**, 51 (2013).

[59] F. A. Grünbaum and M. Pejic, Maximal Parrondo's paradox for classical and quantum Markov chains, Lett. Math. Phys. **106**, 251 (2016).

[60] J. Rajendran and C. Benjamin, Implementing Parrondo's paradox with two-coin quantum walks, R. Soc. Open Sci. **5**, 171599 (2018).

[61] J. Rajendran and C. Benjamin, Playing a true Parrondo's game with a three-state coin on a quantum walk, Europhys. Lett. **122**, 40004 (2018).

[62] J. W. Lai, J. R. A. Tan, H. Lu, Z. R. Yap, and K. H. Cheong, Parrondo paradoxical walk using four-sided quantum coins, Phys. Rev. E **102**, 012213 (2020).

[63] J. W. Lai and K. H. Cheong, Parrondo effect in quantum coin-toss simulations, Phys. Rev. E **101**, 052212 (2020).

[64] M. A. Pires and S. M. D. Queirós, Parrondo's paradox in quantum walks with time-dependent coin operators, Phys. Rev. E **102**, 042124 (2020).

[65] M. Jan, Q.-Q. Wang, X.-Y. Xu, W.-W. Pan, Z. Chen, Y.-J. Han, C.-F. Li, G.-C. Guo, and D. Abbott, Experimental realization of Parrondo's paradox in 1D quantum walks, Adv. Quantum Technol. **3**, 1900127 (2020).

[66] Z. Walczak and J. H. Bauer, Parrondo's paradox in quantum walks with deterministic aperiodic sequence of coins, Phys. Rev. E **104**, 064209 (2021).

[67] Z. Walczak and J. H. Bauer, Parrondo's paradox in quantum walks with three coins, Phys. Rev. E **105**, 064211 (2022).

[68] M. Jan, N. A. Khan, and G. Xianlong, Territories of Parrondo's paradox and its entanglement dynamics in quantum walks, Eur. Phys. J. Plus **138**, 65 (2023).

[69] G. P. Harmer and D. Abbott, A review of Parrondo's paradox, Fluct. Noise Lett. **02**, R71 (2002).

[70] D. Abbott, Asymmetry and disorder: A decade of Parrondo's paradox, Fluct. Noise Lett. **09**, 129 (2010).

[71] K. H. Cheong, J. M. Koh, and M. C. Jones, Paradoxical survival: Examining the Parrondo effect across biology, BioEssays **41**, 1900027 (2019).

[72] J. W. Lai and K. H. Cheong, Social dynamics and Parrondo's paradox: A narrative review, Nonlinear Dyn. **101**, 1 (2020).

[73] J. W. Lai and K. H. Cheong, Parrondo's paradox from classical to quantum: A review, Nonlinear Dyn. **100**, 849 (2020).

[74] Y. Aharonov, L. Davidovich, and N. Zagury, Quantum random walks, Phys. Rev. A **48**, 1687 (1993).

[75] D. A. Meyer, From quantum cellular automata to quantum lattice gases, J. Stat. Phys. **85**, 551 (1996).

[76] R. Portugal, *Quantum Walks and Search Algorithms* (Springer, Cham, 2018).

[77] N. Konno, Quantum random walks in one dimension, Quantum Inf. Process. **1**, 345 (2002).

[78] N. Konno, A new type of limit theorems for the one-dimensional quantum random walk, J. Math. Soc. Jpn. **57**, 1179 (2005).

[79] K. Życzkowski, P. Horodecki, A. Sanpera, and M. Lewenstein, Volume of the set of separable states, Phys. Rev. A **58**, 883 (1998).

[80] G. Vidal and R. F. Werner, Computable measure of entanglement, Phys. Rev. A **65**, 032314 (2002).

[81] G. Abal, R. Siri, A. Romanelli, and R. Donangelo, Quantum walk on the line: Entanglement and nonlocal initial conditions, Phys. Rev. A **73**, 042302 (2006).

[82] M. B. Plenio, Logarithmic negativity: A full entanglement monotone that is not convex, Phys. Rev. Lett. **95**, 090503 (2005).

[83] T. A. Brun, H. A. Carteret, and A. Ambainis, Quantum random walks with decoherent coins, Phys. Rev. A **67**, 032304 (2003).

[84] K. Kadian, S. Garhwal, and A. Kumar, Quantum walk and its application domains: A systematic review, Comput. Sci. Rev. **41**, 100419 (2021).

[85] M. A. Nielsen and I. L. Chuang, *Quantum Computation and Quantum Information* (Cambridge University Press, Cambridge, UK, 2010).